Computer Simulations of Giant Fluctuations

Aleksandar Donev

Courant Institute, *New York University*

IMT12, Madrid, May 2016

Collaborators

- Eric Vanden-Eijden, Courant, New York
- Boyce Griffith, UNC Chapel Hill
- John Bell, Lawrence Berkeley Labs (LBL)
- Alejandro Garcia, San Jose State University
- A number of postdocs and graduate students at Courant and LBL
- A number of experimentalists (Italy, France) present at this meeting.

Fluctuating Hydrodynamics

- The thermal velocity fluctuations are described by the (unsteady) **fluctuating Stokes equation**,

$$\rho\partial_t \mathbf{v} + \boldsymbol{\nabla}\pi = \eta\boldsymbol{\nabla}^2\mathbf{v} + \sqrt{2\eta k_B T}\,\boldsymbol{\nabla}\cdot(\boldsymbol{\sigma}\star\boldsymbol{\mathcal{W}})\,, \quad \text{and } \boldsymbol{\nabla}\cdot\mathbf{v} = 0. \tag{1}$$

  where the **stochastic momentum flux** is spatio-temporal **white noise**,

$$\langle \mathcal{W}_{ij}(\mathbf{r},t)\mathcal{W}^{\star}_{kl}(\mathbf{r}',t')\rangle = (\delta_{ik}\delta_{jl}+\delta_{il}\delta_{jk})\,\delta(t-t')\delta(\mathbf{r}-\mathbf{r}').$$

  and the smoothing kernel $\boldsymbol{\sigma}$ filters out features at scales below a **cutoff scale** σ.

- The **concentration** $c\,(\mathbf{r},t)$ of a **passive tracer** follows an (additive noise) fluctuating advection-diffusion equation,

$$\partial_t c = -\mathbf{u}\cdot\boldsymbol{\nabla}c + \chi_0\boldsymbol{\nabla}^2 c. \tag{2}$$

Giant Fluctuations in Diffusive Mixing

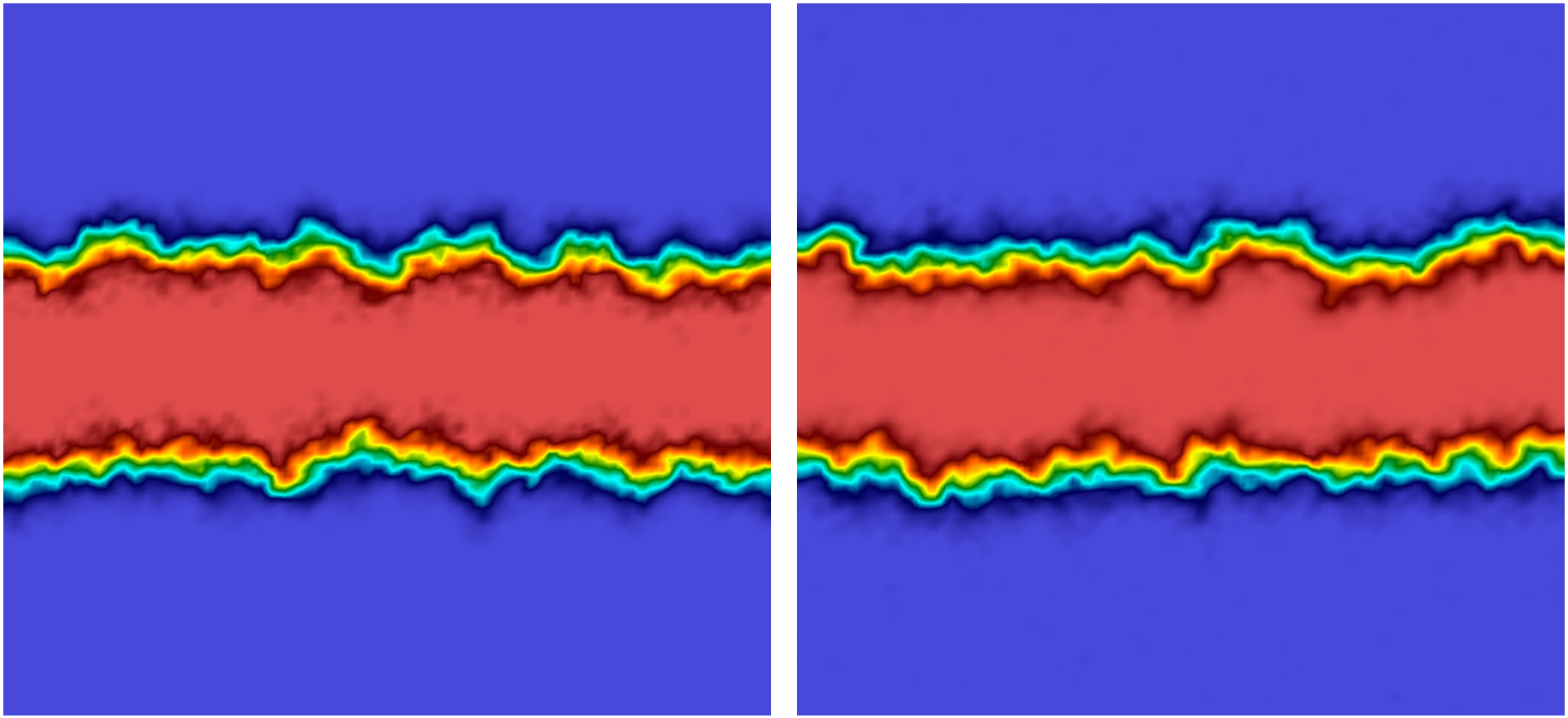

Snapshots of concentration in a miscible mixture showing the development of a *rough* diffusive interface due to the effect of **thermal fluctuations**. These **giant fluctuations** have been studied experimentally and with hard-disk molecular dynamics.

MD vs. Fluct Hydro

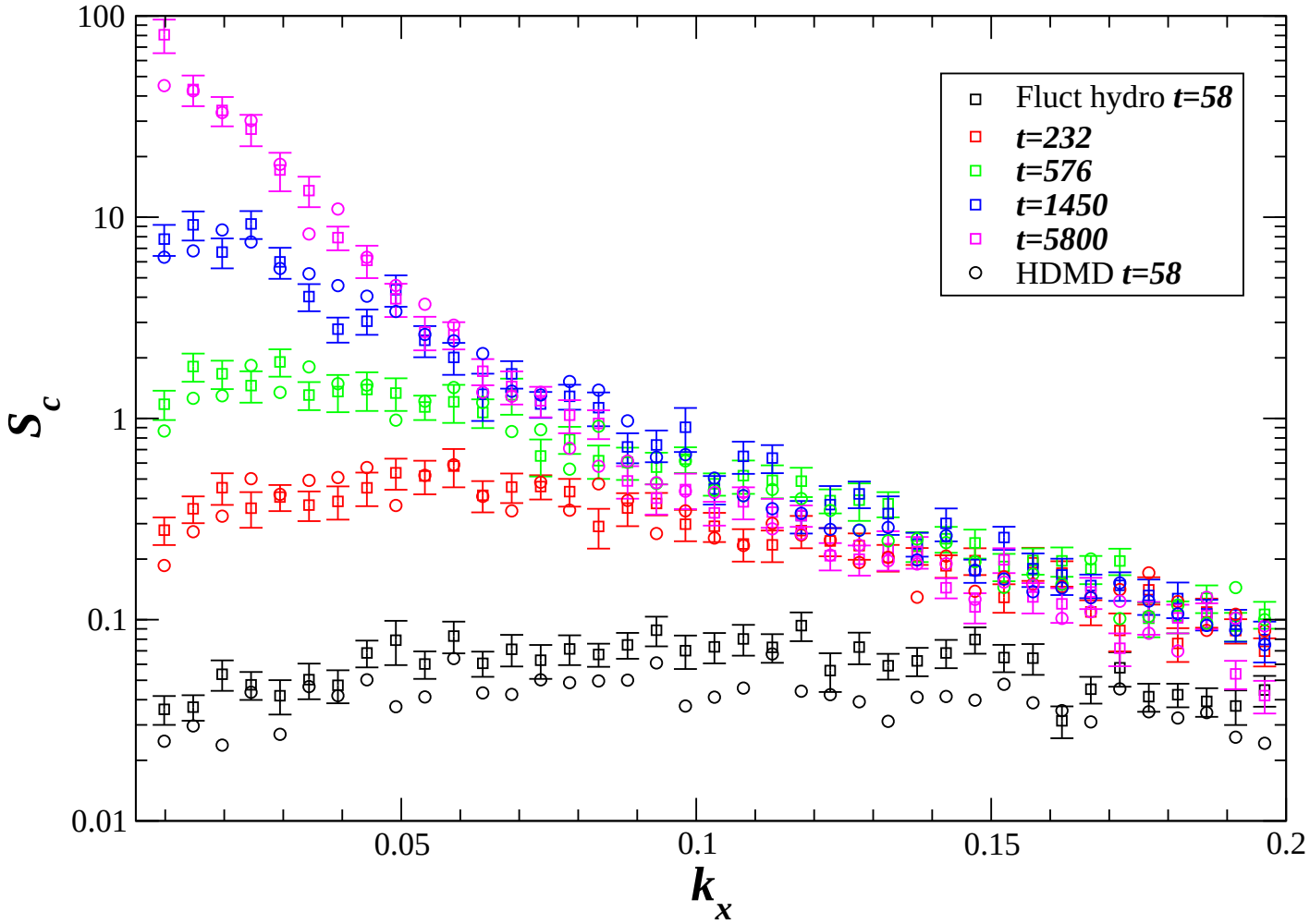

Figure : Discrete spatial spectrum of the interface fluctuations, for fluctuating hydrodynamics (squares) and HD-MD (circles).

Separation of Time Scales

- In liquids molecules are caged (trapped) for long periods of time as they collide with neighbors:
  Momentum and heat diffuse much faster than does mass.
- This means that $\chi \ll \nu$, leading to a **Schmidt number**

$$S_c = \frac{\nu}{\chi} \sim 10^3 - 10^4.$$

  This **extreme stiffness** solving the concentration/tracer equation numerically challenging.
- There exists a **limiting (overdamped) dynamics** for c in the limit $S_c \to \infty$ in the scaling

$$\chi\nu = \text{const.}$$

Overdamped Dynamics

- Adiabatic mode elimination gives the following limiting Ito **stochastic advection-diffusion equation**,

$$\partial_t c = \boldsymbol{\nabla} \cdot [\chi(\mathbf{r}) \boldsymbol{\nabla} c] - \mathbf{w} \cdot \boldsymbol{\nabla} c, \tag{3}$$

  which is **exactly the same as** what was derived from **Brownian dynamics**.
- The advection velocity $\mathbf{w}(\mathbf{r}, t)$ is **white in time**, with covariance proportional to a Green-Kubo integral of the velocity auto-correlation function,

$$\begin{aligned}
\langle \mathbf{w}(\mathbf{r}, t) \otimes \mathbf{w}(\mathbf{r}', t') \rangle &= 2\,\delta(t - t') \int_0^\infty \langle \mathbf{u}(\mathbf{r}, t) \otimes \mathbf{u}(\mathbf{r}', t + t') \rangle dt' \\
&= 2\boldsymbol{\mathcal{R}}(\mathbf{r}, \mathbf{r}')\,\delta(t - t') \\
&= \frac{k_B T}{\eta} \int \boldsymbol{\sigma}(\mathbf{r}, \mathbf{q}')\, \mathbf{G}(\mathbf{r}', \mathbf{r}'')\, \boldsymbol{\sigma}^T(\mathbf{r}'', \mathbf{q}'')\, d\mathbf{q}' d\mathbf{q}'',
\end{aligned}$$

  where $\mathbf{G}$ is the Green's function for steady Stokes flow with the appropriate boundary conditions.

Giant Nonequilibrium Fluctuations

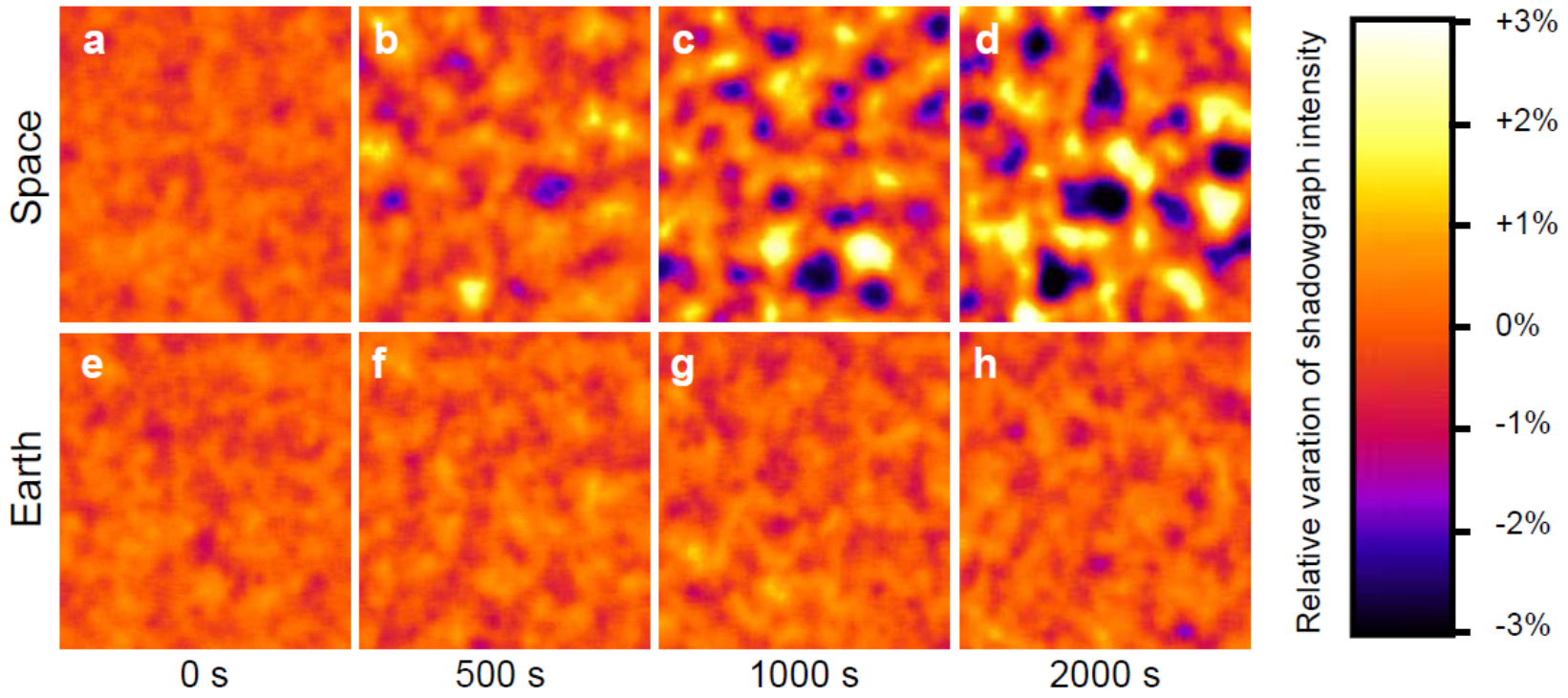

Experimental results by A. Vailati *et al.* from a microgravity environment showing **giant fluctuations** in the concentration of polystyrene in toluene in space (box scale is 5mm on the side, 1mm thick).

Fluctuations become macrosopically large at macroscopic scales!

These come because of **hydrodynamic effects** on diffusion in liquids.

Linearized Fluctuating Hydrodynamics

- When macroscopic gradients are present, steady-state thermal fluctuations become **long-range correlated**.
- Consider a **binary mixture** of fluids and consider **concentration fluctuations** around a macroscopic state $\bar{c}(\mathbf{r}, t)$, $c = \bar{c} + \delta c$.
- The concentration fluctuations are **advected by the random velocities**,

$$\begin{aligned}
\partial_t \bar{c} &= \chi \boldsymbol{\nabla}^2 \bar{c} \\
\partial_t (\delta c) &= -\mathbf{v} \cdot \boldsymbol{\nabla} \bar{c} + \chi \boldsymbol{\nabla}^2 \delta c + \boldsymbol{\nabla} \cdot \left(\sqrt{2\chi \bar{c}}\, \boldsymbol{\mathcal{W}}_c \right) \\
\rho \partial_t \mathbf{v} + \boldsymbol{\nabla} \pi &= \eta \boldsymbol{\nabla}^2 \mathbf{v} - \beta \rho (\delta c)\, \mathbf{g} + \sqrt{2\eta k_B T}\, \boldsymbol{\nabla} \cdot \boldsymbol{\mathcal{W}},
\end{aligned}$$

  where β is the solutal expansion coefficient. This system of SPDEs can easily be solved numerically once we take the **overdamped limit**.
- Note that here χ is the deterministic (Fickian) diffusion coefficient which is *larger* than the bare χ_0.

Back of the Envelope

- The coupled *linearized velocity*-concentration system in **one dimension**:

$$\begin{aligned} v_t &= \nu v_{xx} + \sqrt{2\rho^{-1}\nu}\, W_x \\ c_t &= \chi c_{xx} - v\bar{c}_x, \end{aligned}$$

  where $\bar{c}_x$ is the imposed background concentration gradient.
- The linearized system can be easily solved in Fourier space to give a **power-law divergence** for the spectrum of the concentration fluctuations as a function of wavenumber k,

$$\langle \hat{c}\hat{c}^{\star} \rangle = \rho \frac{k_B T}{\chi(\chi+\nu)k^4} (\bar{c}_x)^2 \approx \frac{k_B T}{\chi\eta k^4} (\bar{c}_x)^2 \text{ for large Sc.}$$

- Concentration fluctuations become **long-ranged** and are **enhanced** as the square of the gradient, to values much larger than equilibrium fluctuations.
- In real life the divergence is **suppressed** by **surface tension**, **gravity**, or **boundaries** (usually in that order).

Simulation versus Theory/Experiment

1. Simulations have the following advantages over analytical theory:
   1. **Numerical linearization** around arbitrary **time-dependent** macroscopic states including **nonlinearities** (e.g., chemistry).
   2. Nontrivial **boundary conditions** can be accounted for relatively easily.
2. Simulations have the following advantages over experiments:
   1. One can easily turn different effects/terms **on and off** to understand what physics is important.
   2. **No measurement noise** or contamination, but still includes thermal fluctuations.
3. Disadvantages of simulations include:
   1. Fluctuations imply **statistical noise**, so long runs needed to compute averages (Monte Carlo).
   2. Cannot easily handle **time and length scale separation**.
   3. Development of computer codes is like developing a new experimental apparatus; it takes time!

GRADFLEX transient

1. We numerically solve the equations

$$\rho\partial_t \mathbf{v} + \boldsymbol{\nabla}\pi = \eta\boldsymbol{\nabla}^2\mathbf{v} + \boldsymbol{\nabla}\cdot\left(\sqrt{2\eta k_B T_0}\,\boldsymbol{\mathcal{W}}\right) \tag{4}$$

$$\boldsymbol{\nabla}\cdot\mathbf{v} = 0$$

$$\partial_t c + \mathbf{v}\cdot\boldsymbol{\nabla}c = D\boldsymbol{\nabla}\cdot\left(\boldsymbol{\nabla}c + c\,(1-c)\,S_T\boldsymbol{\nabla}T\right) \tag{5}$$

$$\partial_t T + \mathbf{v}\cdot\boldsymbol{\nabla}T = \kappa\boldsymbol{\nabla}^2 T, \tag{6}$$

2. Our numerical methods perform **numerical linearization** by solving the fully nonlinear equations with weak noise.
3. In the linearized regime **no difference between 2D and 3D** so we sometimes solve 2D equations to speed up computations.
4. Numerically we **separately solve** (4,5) for concentration (overdamped), and we separately solve (4,6) for temperature (inertial) [1].

Overdamped Temporal Integrator

The limiting dynamics can be efficiently simulated using the following **predictor-corrector algorithm** (implemented on GPUs):

1. Generate a random advection velocity by solving **steady Stokes** with random forcing,

$$\boldsymbol{\nabla}\pi^{n+\frac{1}{2}} = \nu\left(\boldsymbol{\nabla}^2\mathbf{v}^n\right) + \Delta t^{-\frac{1}{2}}\boldsymbol{\nabla}\cdot\left(\sqrt{2\nu\rho^{-1}\,k_B\,T}\,\boldsymbol{\mathcal{W}}^n\right) - \rho\beta c^n\mathbf{g}$$

$$\boldsymbol{\nabla}\cdot\mathbf{v}^n = 0.$$

   using a staggered **finite-volume** fluctuating hydrodynamics solver.

2. Do a **predictor advection-diffusion solve** for concentration,

$$\frac{\tilde{c}^{n+1} - c^n}{\Delta t} = -\mathbf{v}^n\cdot\boldsymbol{\nabla}c^n + \chi_0\boldsymbol{\nabla}^2\left(\frac{c^n + \tilde{c}^{n+1}}{2}\right).$$

contd.

1. Solve a **corrector** steady Stokes system for **velocity**,

$$\boldsymbol{\nabla}\pi^{n+\frac{1}{2}} = \eta\left(\boldsymbol{\nabla}^2\mathbf{v}^{n+\frac{1}{2}}\right) + \boldsymbol{\nabla}\cdot\left(\sqrt{\frac{2\eta\, k_B T}{\Delta t \Delta V}}\,\mathbf{W}^n\right) - \rho\beta\left(\frac{c^n + \tilde{c}^{n+1}}{2}\right)\mathbf{g}$$

$$\boldsymbol{\nabla}\cdot\mathbf{v}^{n+\frac{1}{2}} = 0.$$

2. Take a **corrector** step for **concentration**,

$$\frac{c^{n+1} - c^n}{\Delta t} = -\mathbf{v}^{n+\frac{1}{2}}\cdot\boldsymbol{\nabla}\left(\frac{c^n + \tilde{c}^{n+1}}{2}\right) + \chi_0\boldsymbol{\nabla}^2\left(\frac{c^n + c^{n+1}}{2}\right).$$

This overdamped integrator provides a speedup of $O(\mathrm{Sc})$ over direct integration of the original inertial equations.

Comparison to GRADFLEX transient

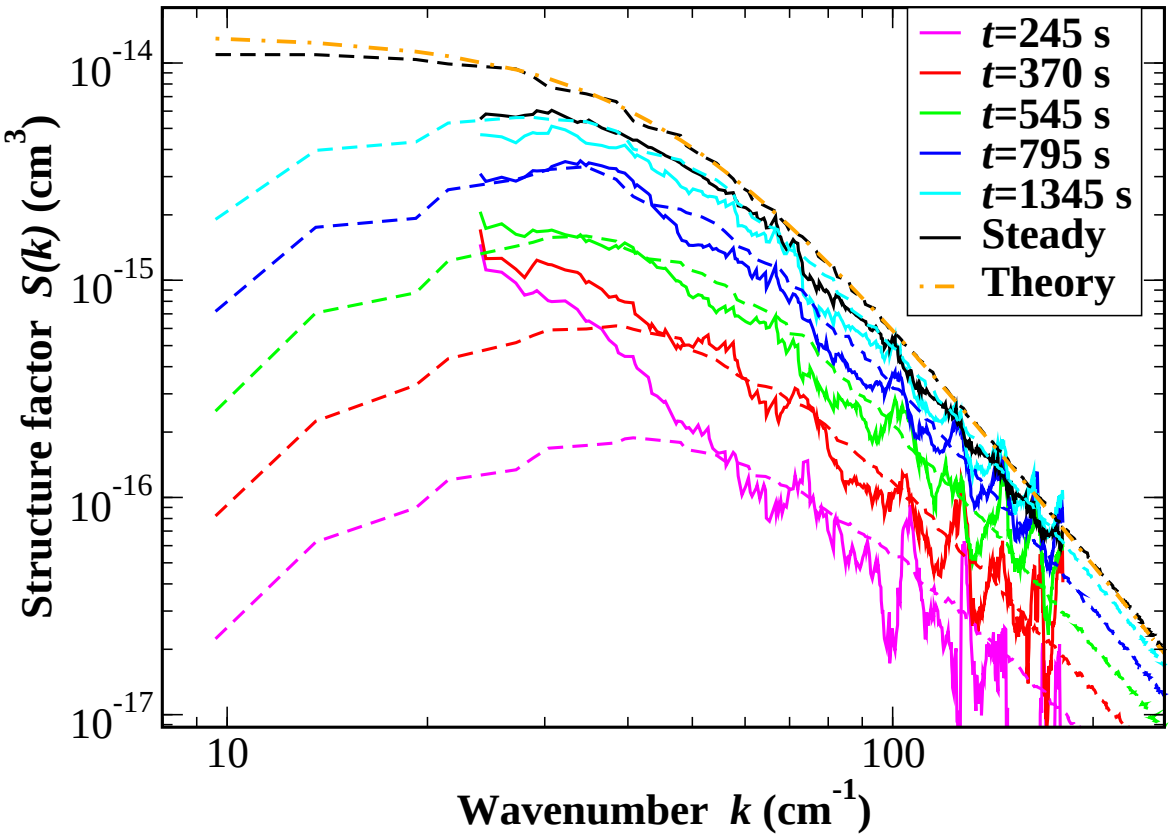

Figure : **Qualitative theory** [2]: $S(k,t) \propto [1 - \exp(-2Dk^2 t)]S(k,\infty)$

Relaxation times in confinement

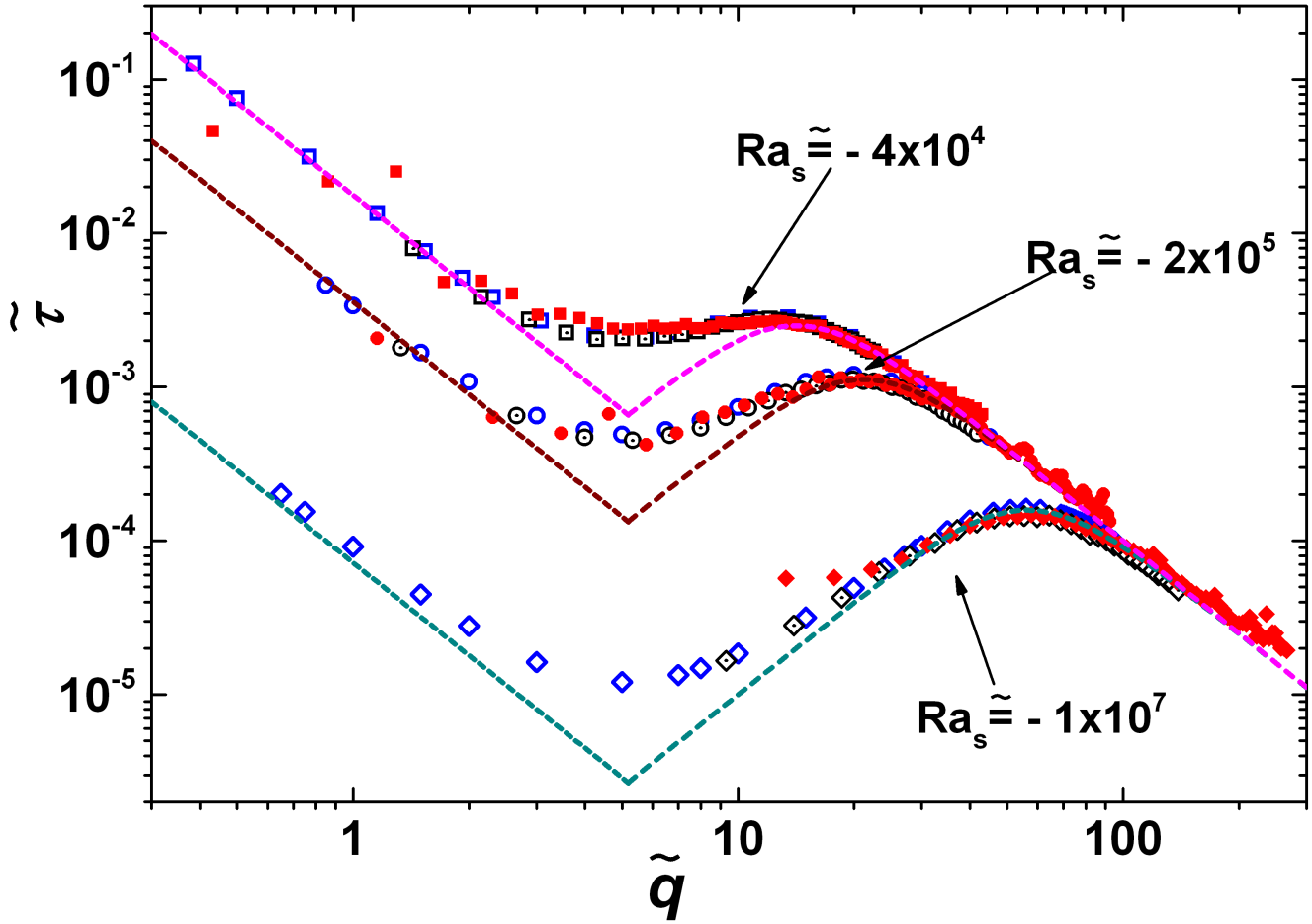

Figure : Dimensionless effective decay times $\tilde{\tau}$ as a function of dimensionless wave number $\tilde{q}$ [3]. Filled red markers are experimental data, open blue are for calculations based on the FHD model, and open-dotted black are from numerical simulations.

Where does overdamped apply?

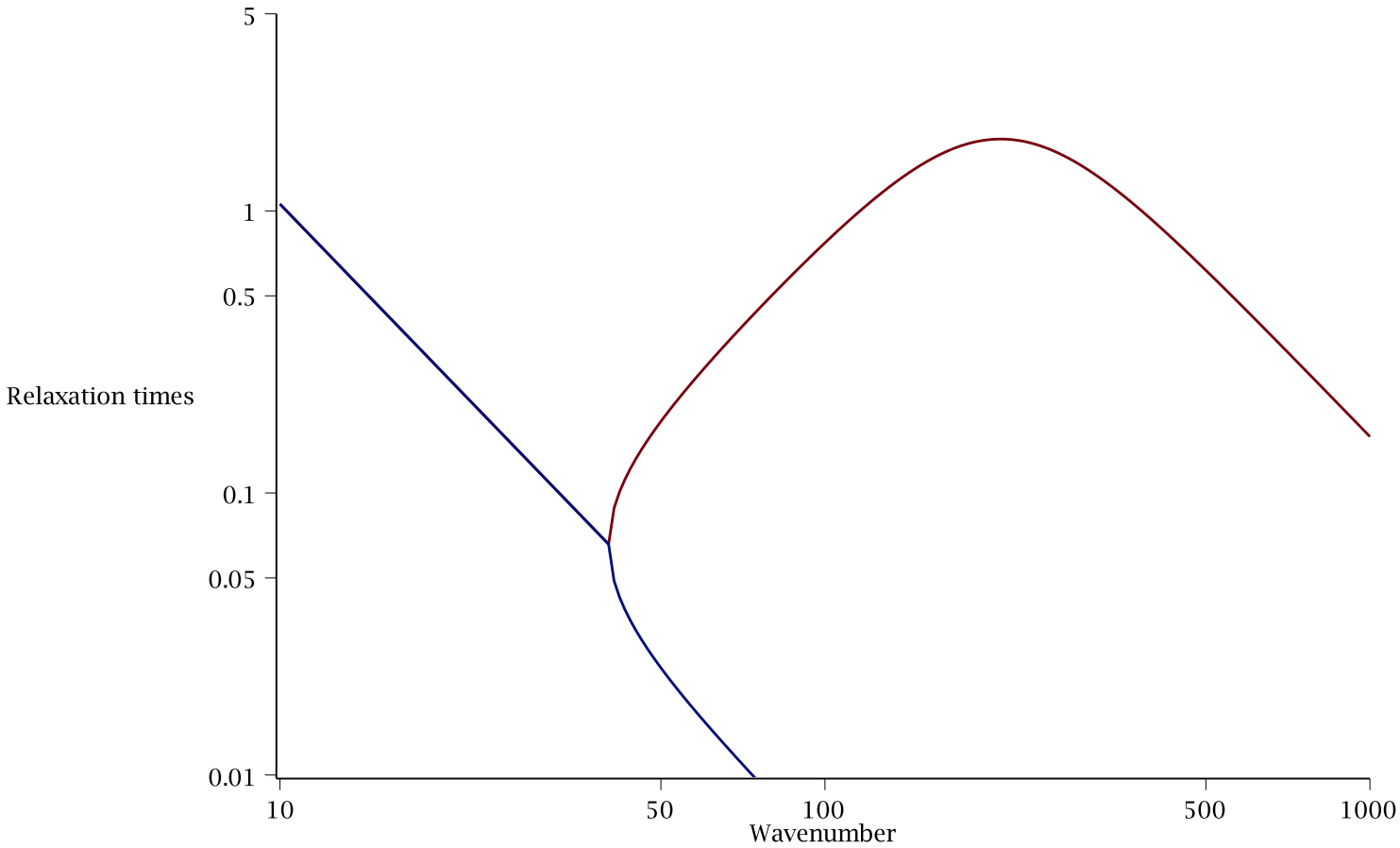

Figure : The overdamped limit is only good for wavenumbers above 50cm^{-1}. At even larger scales **fluid inertia cannot be neglected** when there is gravity present.

Propagative Modes

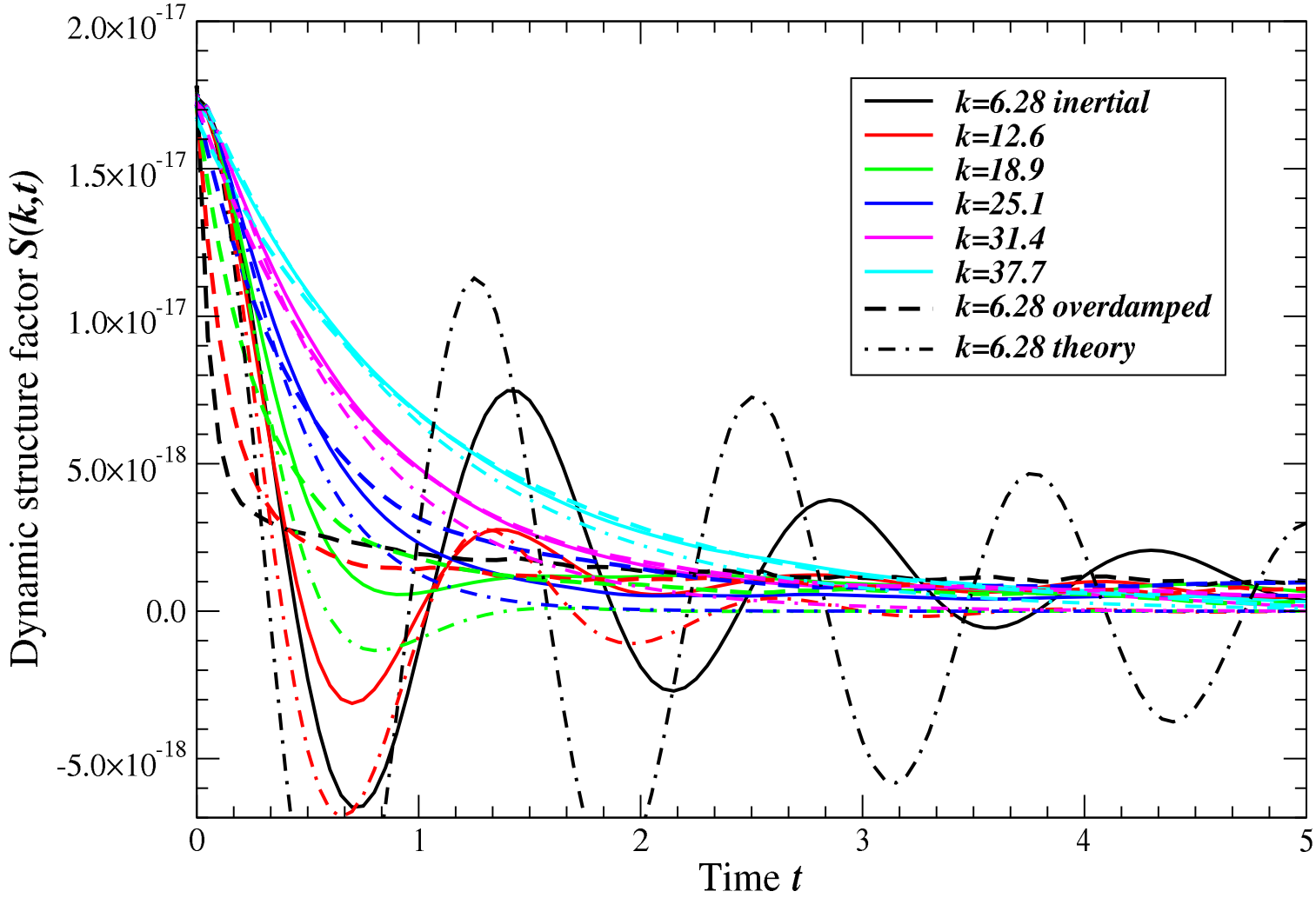

Figure : (Color online) Propagative modes (gravity waves) [1] appear in the inertial equations (dotted), but not overdamped (dashed).

Complex Fluids

We have generalized the models and numerical codes to include more complex fluids:

- **Multispecies mixtures** with complete transport including **thermo and barodiffusion** and boundary conditions and gravity [4]. We have simulated the development of gravity-driven diffusive instabilities and compared to experiments.
- **Chemically-reacting mixtures** [5]. We have studied giant fluctuations in reactive mixtures and found that the nonlinearity of the base (macroscopic) state is crucial and not yet captured in theory.
- **Multiphase liquids** including liquid-vapor coexistence [6]. We have simulated capillary waves, spinodal decomposition, condensation, and the piston effect.
- **Ionic mixtures** including electrostatic effects at length scales comparable to the Debye length (in preparation).

Chemically-Reactive Mixtures

- The species density equations for a mixture of N_{S} species are given by

$$\frac{\partial}{\partial t}\left(\rho_s\right) + \nabla \cdot \left(\rho_s \mathbf{v} + \mathbf{F}\right) = m_s \Omega_s, \qquad \left(s = 1, \ldots N_{\mathrm{S}}\right) \tag{7}$$

- Due to mass conservation $\rho = \sum_s \rho_s$ follows the continuity equation,

$$\frac{\partial}{\partial t}\rho + \nabla \cdot \left(\rho \mathbf{v}\right) = 0. \tag{8}$$

- The mass fluxes take the form, excluding barodiffusion and thermodiffusion,

$$\mathbf{F} = \rho \mathbf{W} \left[\chi \boldsymbol{\Gamma} \boldsymbol{\nabla} \mathbf{x} + \sqrt{\frac{2}{n}} \chi^{\frac{1}{2}} \boldsymbol{\mathcal{W}}_F \left(\mathbf{r}, t\right) \right],$$

where n is the number density, x_s is the mole fraction of species s, and $\mathbf{W} = \mathrm{Diag}\left\{w_s = \rho_s/\rho\right\}$ contains the mass fractions.

Multispecies Mass Diffusion

- $\mathbf{\Gamma}$ is a matrix of thermodynamic factors,

$$\mathbf{\Gamma} = \mathbf{I} + \left(\mathbf{X} - \mathbf{x}\mathbf{x}^T\right)\left(\frac{\partial^2 g_{\text{ex}}}{\partial \mathbf{x}^2}\right),$$

  where $g_{\text{ex}}(\mathbf{x}, T, P)$ is the normalized **excess Gibbs energy density** per particle.

- χ is an **SPD diffusion tensor** that can be related to the **Maxwell-Stefan diffusion coefficients** and Green-Kubo type formulas.

- We, however, do not know values of these for even a single ternary mixture!

  We have studied **ideal mixtures**: hard-sphere **gas mixtures [7]** and **dilute solutions** of salt+sugar in water [4].

Chemical Reactions

- Consider a system with N_{R} **elementary reactions** with reaction r

$$\mathfrak{R}_r : \qquad \sum_{s=1}^{N_{\mathrm{S}}} \nu_{sr}^{+} \mathfrak{M}_s \rightleftarrows \sum_{s=1}^{N_{\mathrm{S}}} \nu_{sr}^{-} \mathfrak{M}_s$$

  The **stoichiometric coefficients** are $\nu_{sr} = \nu_{sr}^{-} - \nu_{sr}^{+}$ and mass conservation requires that $\sum_s \nu_{sr} m_r = 0$.
- Define the dimensionless **chemical affinity**

$$\mathcal{A}_r = \sum_s \nu_{sr}^{+} \hat{\mu}_s - \sum_s \nu_{sr}^{-} \hat{\mu}_s,$$

  where $\hat{\mu}_s = m_s \mu_s / k_B T$ is the dimensionless **chemical potential per particle**.
- Also define the **thermodynamic driving force**

$$\hat{\mathcal{A}}_r = \exp\left(\sum_s \nu_{sr}^{+} \hat{\mu}_s\right) - \exp\left(\sum_s \nu_{sr}^{-} \hat{\mu}_s\right) = \prod_s e^{\nu_{sr}^{+} \hat{\mu}_s} - \prod_s e^{\nu_{sr}^{-} \hat{\mu}_s}$$

Chemical Langevin Equation

- The mass production due to chemistry can be approximated by the chemical Langevin equation (CLE) [5]:

$$\Omega_s = \sum_r \nu_{sr} \left(\frac{P}{\tau_r k_B T} \right) \hat{\mathcal{A}}_r + \sum_r \nu_{sr} \left(\frac{P}{\tau_r k_B T} \prod_s e^{\nu_{sr}^+ \hat{\mu}_s} \right)^{\frac{1}{2}} \mathcal{Z}(\mathbf{r}, t) \tag{9}$$

- The **CLE** follows from a truncation of the Kramers-Moyal expansion at second order.
  No true thermodynamic equilibrium since it assumes **one-way reactions**.
- The CLE is **not time-reversible** (obeys detailed balance) **at thermodynamic equilibrium** wrt to the Einstein distribution.
  Proper description of chemical reactions requires the use of SDEs driven by **Poisson noise** (not Gaussian).

Nonlinear Chemical Networks

We have studied the Baras-Pearson-Mansour (BPM) model $\mathfrak{M} = (U, V, W, S, U_f, V_f)$,

$$\begin{aligned} \mathfrak{R}_1 : &\quad U + W \leftrightarrows V + W \\ \mathfrak{R}_2 : &\quad V + V \leftrightarrows W + S \\ \mathfrak{R}_3 : &\quad V \leftrightarrows S \\ \mathfrak{R}_4 : &\quad U \leftrightarrows U_f \\ \mathfrak{R}_5 : &\quad V \leftrightarrows V_f \end{aligned} \tag{10}$$

This system can exhibit **limit cycles**, bimodal states (**bistability**), and possibly other nonlinear behavior.
In principle this system can be simulated using **particle methods**!

Turing-like Patterns

Fluctuations change the dynamics **qualitatively** in spatially-extended reactive systems! **How do we simulate this?**

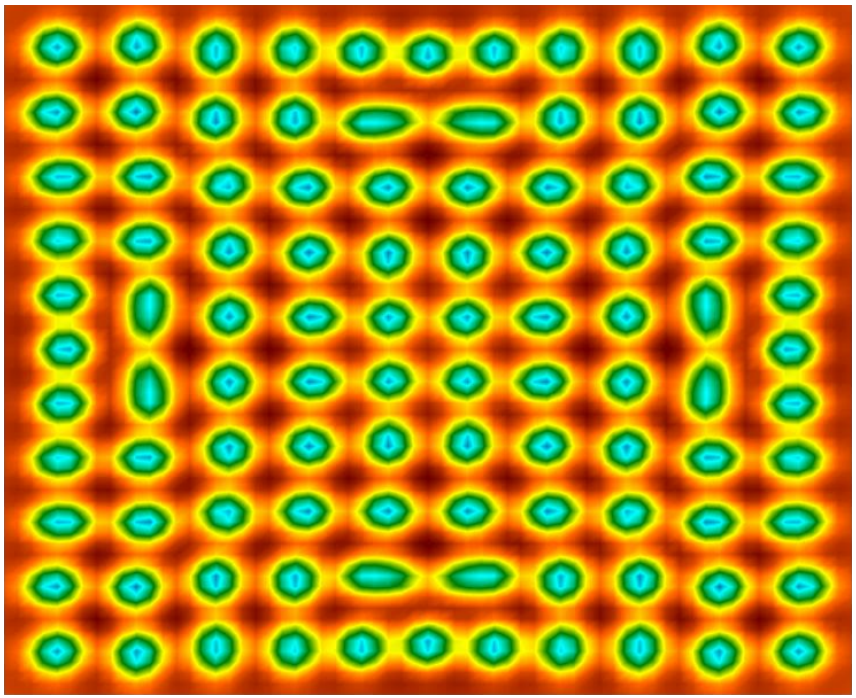

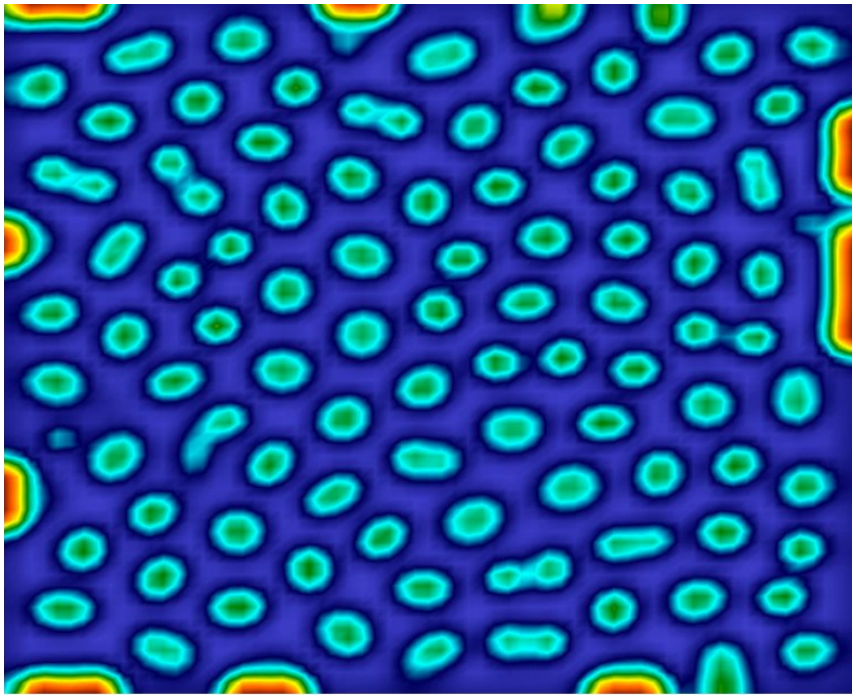

Multiphase Systems: Liquid-Vapor

- We will use a **diffusive-interface model** for describing interfaces between two distinct phases such as liquid and vapor of a single species.
- Coarse-grained free energy follows the usual **square-gradient surface tension model**

$$F\left(\rho(\mathbf{r}), \nabla\rho(\mathbf{r}), T(\mathbf{r})\right) = \int \mathrm{d}\mathbf{r} \left(f\left(\rho(\mathbf{r}), T(\mathbf{r})\right) + \frac{1}{2}\kappa \left|\nabla\rho(\mathbf{r})\right|^2 \right) \quad (11)$$

  The **local free energy density** $f\left(\rho(\mathbf{r}), T(\mathbf{r})\right)$ includes the hard-core repulsions as well as the short-range attractions.
- Assume a **van der Waals** loop for the equation of state,

$$P\left(\rho, T\right) = \frac{nk_B T}{1 - b'n} - a'n^2, \quad (12)$$

$$f = nk_B T \ln\left[\frac{\rho}{1 - b'n}\right] - a'n^2.$$

Fluctuating Hydrodynamics

$$\partial_t \rho + \nabla \cdot (\rho \mathbf{v}) = 0 \tag{13}$$

$$\partial_t (\rho \mathbf{v}) + \nabla \cdot \left(\rho \mathbf{v}\mathbf{v}^{\mathrm{T}}\right) + \nabla \cdot \mathbf{\Pi} = \nabla \cdot (\boldsymbol{\sigma} + \mathbf{\Sigma}) \tag{14}$$

$$\partial_t (\rho E) + \nabla \cdot (\rho E \mathbf{v} + \mathbf{\Pi} \cdot \mathbf{v}) = \nabla \cdot (\psi + \mathbf{\Psi}) + \nabla \cdot ((\boldsymbol{\sigma} + \mathbf{\Sigma}) \cdot \mathbf{v}), \tag{15}$$

where the momentum density is $\mathbf{g} = \rho \mathbf{v}$ and
the total local energy density is $\rho E = \frac{1}{2}\rho v^2 + \rho e$.

Momentum Fluxes

- The reversible contribution to the stress tensor is [6]

$$\mathbf{\Pi} = P\mathbf{I} - \left[\left(\kappa\rho\nabla^2\rho + \frac{1}{2}\kappa\left|\nabla\rho\right|^2\right)\mathbf{I}\right] - \left(\kappa\nabla\rho\otimes\nabla\rho\right) + \text{cross term?}$$

- Irreversible contribution to the stress is the viscous stress tensor

$$\boldsymbol{\sigma} = \eta\left(\nabla\mathbf{v} + (\nabla\mathbf{v})^{\mathrm{T}}\right) + \left(\zeta - \frac{2}{3}\eta\right)(\nabla\cdot\mathbf{v})\,\mathbf{I} \tag{16}$$

- Stochastic stress tensor obeys fluctuation-dissipation balance

$$\mathbf{\Sigma} = \sqrt{2\eta k_B T}\,\widetilde{\boldsymbol{\mathcal{W}}} + \left(\sqrt{\frac{\zeta k_B T}{3}} - \sqrt{\frac{2\eta k_B T}{3}}\right)\mathrm{Tr}\left(\widetilde{\boldsymbol{\mathcal{W}}}\right)\mathbf{I}, \tag{17}$$

where $\widetilde{\boldsymbol{\mathcal{W}}} = (\boldsymbol{\mathcal{W}} + \boldsymbol{\mathcal{W}}^T)/\sqrt{2}$ is a symmetric white-noise tensor field.

Capillary Waves

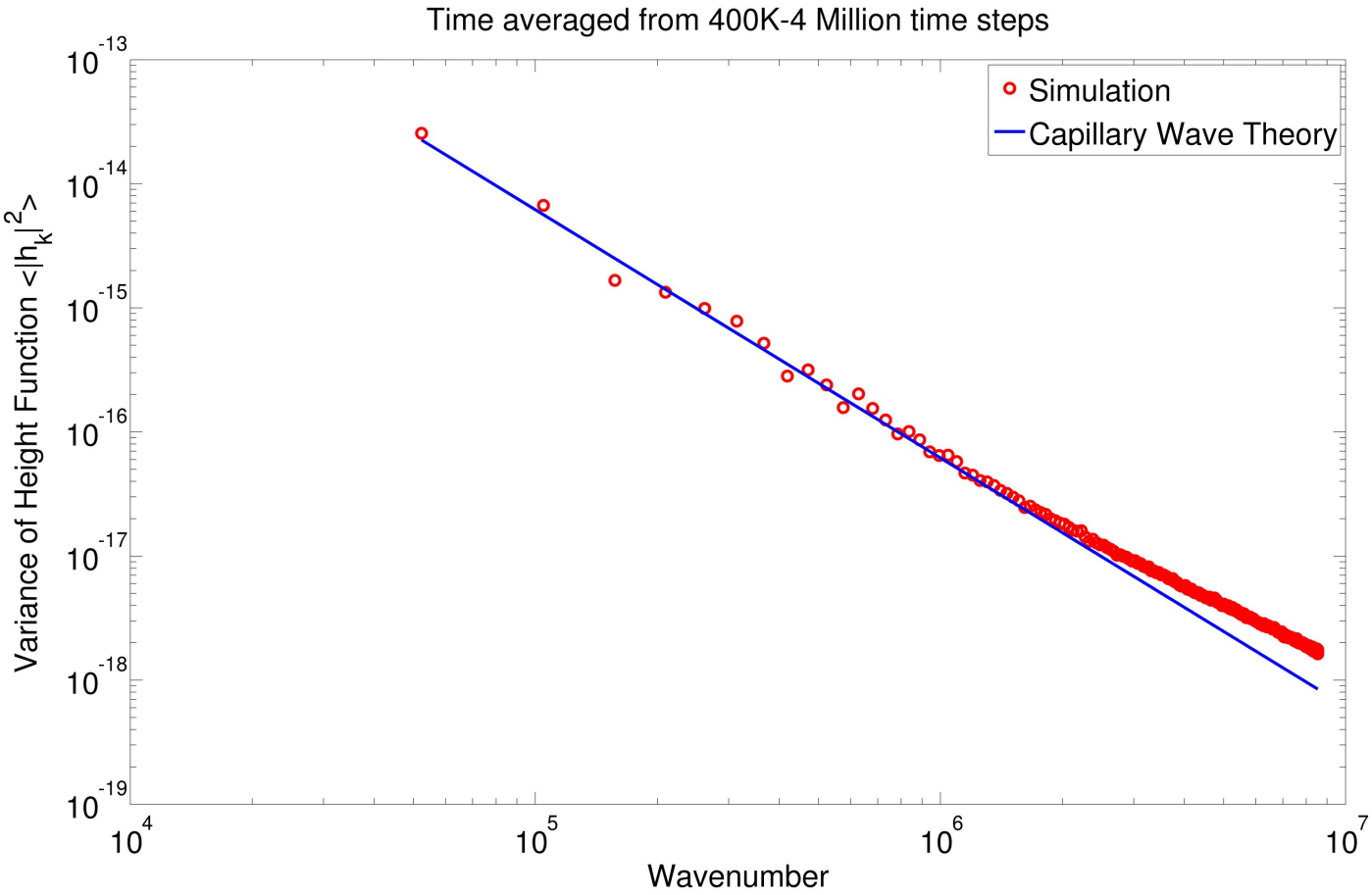

Variance of height fluctuations versus wavenumber comparing 2D simulations (red circles) and **capillary wave theory** (CWT) (black solid line).

Spinodal Decomposition

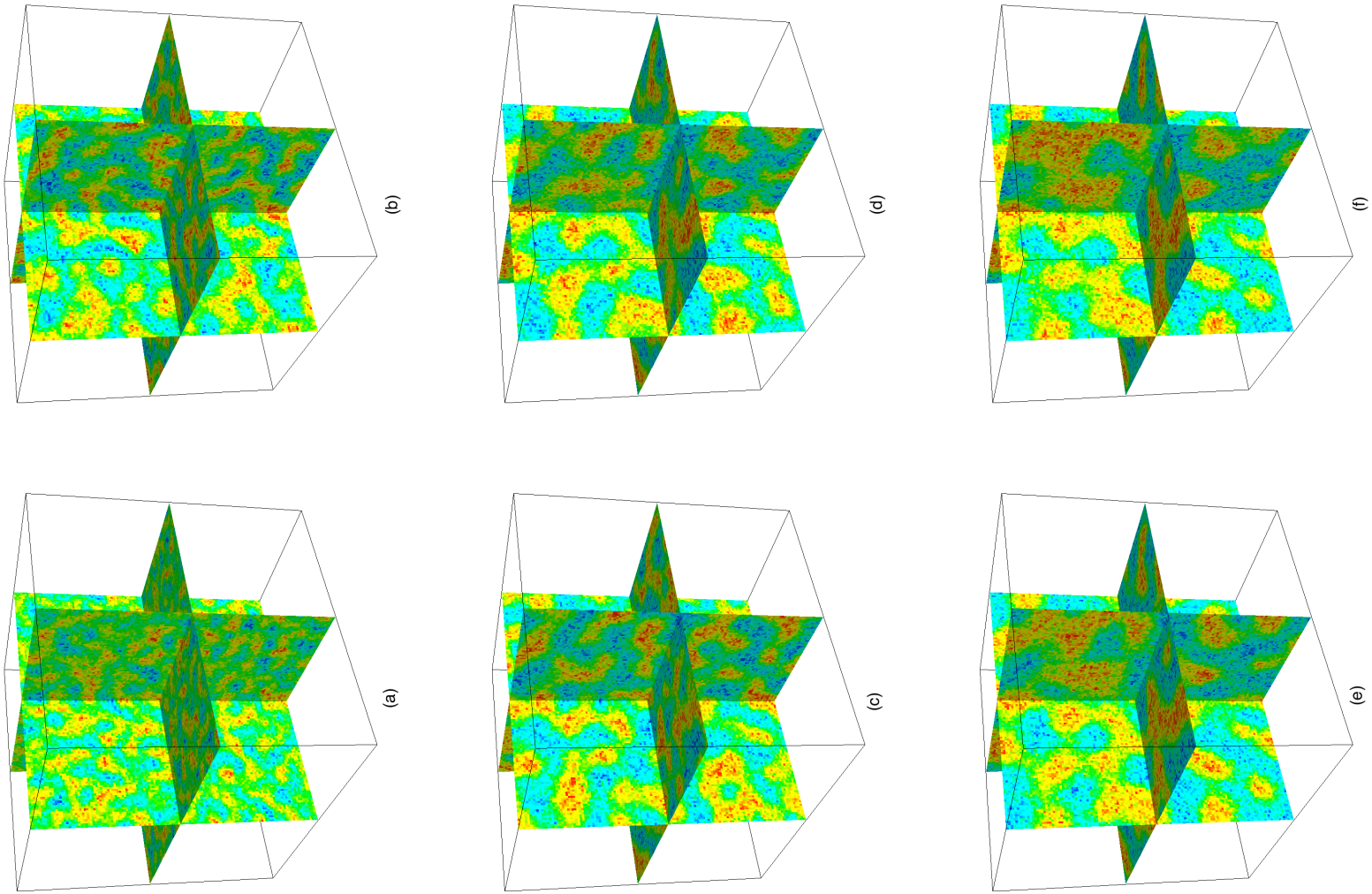

Spinodal decomposition in a near-critical Argon system at $\rho = 0.416$ g/cc, $T = 145.85$ K leading to a **bicontinuous pattern**.

Condensation

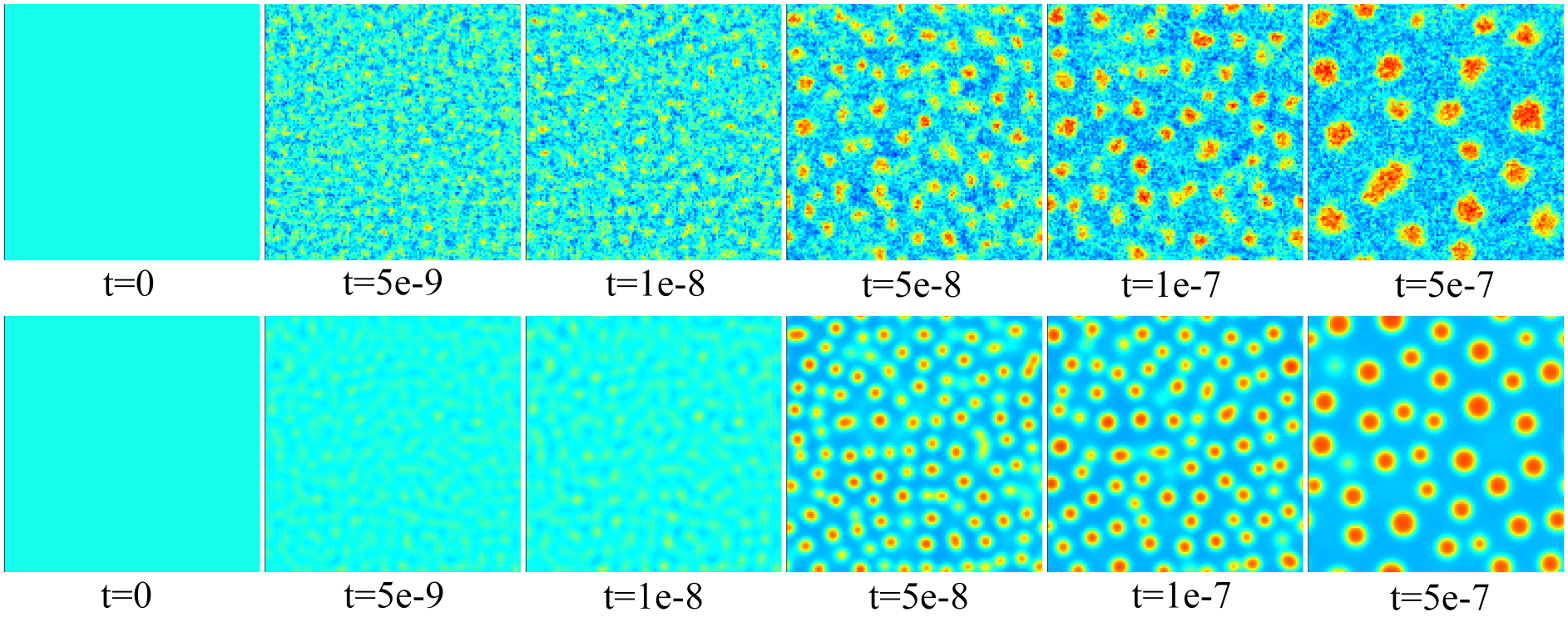

Liquid-vapor spinodal decomposition in a near-critical van der Waals Argon system at $\rho = 0.36\ \mathrm{g/cc}$, $T = 145.85\ \mathrm{K}$ leading to **droplets** forming in a majority vapor phase.

References

S. Delong, Y. Sun, B. E. Griffith, E. Vanden-Eijnden, and A. Donev.
Multiscale temporal integrators for fluctuating hydrodynamics.
Phys. Rev. E, 90:063312, 2014.
Software available at `https://github.com/stochasticHydroTools/MixingIBAMR`.

A. Donev R. Cerbino, Y. Sun and A. Vailati.
Dynamic scaling for the growth of non-equilibrium fluctuations during thermophoretic diffusion in microgravity.
Scientific Reports, 5, 2015.
Software available at `https://github.com/stochasticHydroTools/MixingIBAMR`.

C. Giraudet, H. Bataller, Y. Sun, A. Donev, J. M. Ortiz de ZÃ¡rate, and F. Croccolo.
Slowing-down of non-equilibrium concentration fluctuations in confinement.
EPL (Europhysics Letters), 111(6):60013, 2015.
Software available at `https://github.com/stochasticHydroTools/MixingIBAMR`.

A. Donev, A. J. Nonaka, A. K. Bhattacharjee, A. L. Garcia, and J. B. Bell.
Low Mach Number Fluctuating Hydrodynamics of Multispecies Liquid Mixtures.
Physics of Fluids, 27(3):037103, 2015.

A. K. Bhattacharjee, K. Balakrishnan, A. L. Garcia, J. B. Bell, and A. Donev.
Fluctuating hydrodynamics of multispecies reactive mixtures.
J. Chem. Phys., 142(22):224107, 2015.

A. Chaudhri, J. B. Bell, A. L. Garcia, and A. Donev.
Modeling multiphase flow using fluctuating hydrodynamics.
Phys. Rev. E, 90:033014, 2014.

K. Balakrishnan, A. L. Garcia, A. Donev, and J. B. Bell.
Fluctuating hydrodynamics of multispecies nonreactive mixtures.
Phys. Rev. E, 89:013017, 2014.